

Research Paper

TRPV4 inhibition prevents paclitaxel-induced neurotoxicity in preclinical models



Wolfgang Boehmerle^{a,b,c,*}, Petra Huehnchen^{a,b,c,1}, Sabrina Lin Lin Lee^{b,d},
Christoph Harms^{a,b,c,d,1}, Matthias Endres^{a,b,c,d,e,f,1}

^a Charité – Universitätsmedizin Berlin, Corporate Member of Freie Universität Berlin, Humboldt-Universität zu Berlin and Berlin Institute of Health, Klinik und Hochschulambulanz für Neurologie, Berlin, Germany

^b Charité – Universitätsmedizin Berlin, Corporate Member of Freie Universität Berlin, Humboldt-Universität zu Berlin and Berlin Institute of Health, Cluster of Excellence NeuroCure, Berlin, Germany

^c Berlin Institute of Health, Anna-Louisa-Karsch 2, 10178 Berlin, Germany

^d Charité – Universitätsmedizin Berlin, Corporate Member of Freie Universität Berlin, Humboldt-Universität zu Berlin and Berlin Institute of Health, Center for Stroke Research Berlin, Berlin, Germany

^e German Center for Neurodegenerative Diseases (DZNE), Berlin, Germany

^f DZHK (German Center for Cardiovascular Research), Berlin, Germany

ARTICLE INFO

Keywords:

Paclitaxel
Neuropathy
Calcium
TRPV4
Inositol-trisphosphate receptor

ABSTRACT

Paclitaxel is a cytotoxic drug which frequently causes sensory peripheral neuropathy in patients. Increasing evidence suggests that altered intracellular calcium (Ca^{2+}) signals play an important role in the pathogenesis of this condition. In the present study, we examined the interplay between Ca^{2+} release channels in the endoplasmic reticulum (ER) and Ca^{2+} permeable channels in the plasma membrane in the context of paclitaxel mediated neurotoxicity. We observed that in small to medium size dorsal root ganglia neurons (DRGN) the inositol-trisphosphate receptor (InsP₃R) type 1 was often concentrated in the periphery of cells, which is in contrast to homogenous ER distribution. G protein-coupled designer receptors were used to further elucidate phosphoinositide mediated Ca^{2+} signaling: This approach showed strong InsP₃ mediated Ca^{2+} signals close to the plasma membrane, which can be amplified by Ca^{2+} entry through TRPV4 channels. In addition, our results support a physical interaction and partial colocalization of InsP₃R1 and TRPV4 channels. In the context of paclitaxel-induced neurotoxicity, blocking Ca^{2+} influx through TRPV4 channels reduced cell death in cultured DRGN. Pretreatment of mice with the pharmacological TRPV4 inhibitor HC067047 prior to paclitaxel injections prevented electrophysiological and behavioral changes associated with paclitaxel-induced neuropathy.

In summary, these results underline the relevance of TRPV4 signaling for the pathogenesis of paclitaxel-induced neuropathy and suggest novel preventive strategies.

1. Introduction

Paclitaxel (PTX) is a cytotoxic drug commonly used in the treatment of solid tumors. One frequent non-hematological side effect of PTX is the development of a painful sensory peripheral neuropathy which not only increases the burden of disease, but frequently also proves to be dose limiting and thus detrimental to therapy (reviewed by (Mielke et al., 2006)). Despite intense research efforts, both in the clinical and the basic sciences, this phenomenon and its underlying

pathomechanisms are still not fully understood and current treatment options are inadequate. A number of recent studies suggest, that an impaired intracellular calcium (Ca^{2+}) homeostasis may play a major role in the pathophysiology of paclitaxel-induced peripheral neurotoxicity and presents a potential therapeutic target: It was shown, that the Ca^{2+} permeable nonselective cation channel transient receptor potential subfamily V member 4 (TRPV4), a receptor which is located in the plasma membrane, is essential for the development of paclitaxel-induced neuropathy in rats (Alessandri-Haber et al., 2008; Alessandri-

Abbreviations: AC, Adenylate cyclase; Ca^{2+} , Calcium; CIPN, Chemotherapy induced neuropathy; CNO, Clozapine-n-oxide; DREADD, Designer receptor exclusively activated by a designer drug; DRGN, Dorsal root ganglia neurons; ER, Endoplasmic reticulum; GPCR, G protein-coupled receptor; InsP₃R, Inositol 1,4,5-trisphosphate receptor; PLA, Proximity ligation assay; RYR, Ryanodine receptors; TRPV4, Transient receptor potential cation channel subfamily V member 4.

* Corresponding author at: Charité Universitätsmedizin Berlin, Klinik und Hochschulambulanz für Neurologie, Chariteplatz 1, Berlin 10117, Germany.

E-mail address: wolfgang.boehmerle@charite.de (W. Boehmerle).

¹ These authors contributed equally to the present manuscript.

<https://doi.org/10.1016/j.expneurol.2018.04.014>

Received 1 December 2017; Received in revised form 17 April 2018; Accepted 27 April 2018

Available online 30 April 2018

0014-4886/ © 2018 Elsevier Inc. All rights reserved.

Haber et al., 2004). This is interesting, as gain-of-function TRPV4 mutations cause the hereditary axonal neuropathy Charcot Marie Tooth disease type 2C (Klein et al., 2011). In addition to TRPV4, other studies implicated the Ca^{2+} permeable channels TRPA1 and TRPV1 in the development of neuropathic pain after PTX treatment in vivo (Chen et al., 2011; Materazzi et al., 2012; Wu et al., 2015). However, it remains unclear if these channels play a role in the pathophysiology of neuropathy development or whether these channels only contribute to the development of symptoms of sensory neuropathy at a later stage, such as mechanical and thermal allodynia. Other reports showed protective effects of the Ca^{2+} channel blocker ethosuximide (Flatters and Bennett, 2004) and various drugs that decrease extra- and intracellular Ca^{2+} levels (Siau and Bennett, 2006). Furthermore, inhibition of the Ca^{2+} -activated protease calpain prevented paclitaxel-induced neuropathy in vivo (Wang et al., 2004).

Alterations of intracellular Ca^{2+} signaling involving the InsP_3R receptor were previously shown in neuronal cells treated with paclitaxel by a number of authors (among others: (Boehmerle et al., 2006; Boehmerle et al., 2007; Pease-Raissi et al., 2017)). Interestingly, chronic changes in Ca^{2+} signaling compatible with some of these observations were also reported in paclitaxel treated animals (Yilmaz and Gold, 2015). In our experiments, we observed an early impairment of the intracellular Ca^{2+} homeostasis in cellular models of paclitaxel-induced neurotoxicity: PTX binds to the protein neuronal calcium sensor-1 (NCS1), stabilizing this protein in its Ca^{2+} bound conformation. At least in part, increased Ca^{2+} signaling occurs through the binding of the PTX-NCS1 complex to the inositol-trisphosphate receptor (InsP_3R) (Schlecker et al., 2006), effecting a positive modulation of the InsP_3R and subsequently increased Ca^{2+} release from the endoplasmic reticulum (ER) (Boehmerle et al., 2006). Interference with this cascade is a promising target for the development of a preventive treatment of paclitaxel-induced neurotoxicity (Huehnchen et al., 2017; Mo et al., 2012). However, these findings do not address the pathophysiological relevance of Ca^{2+} entry across the plasma membrane, as suggested by the studies mentioned above. One potential link between these possibly complementary pathways has been observed in epithelial cells, where it was shown that InsP_3R type 3 binds to TRPV4 channels through a calmodulin-binding site and thus mediates an InsP_3 -dependent sensitization of TRPV4 (Fernandes et al., 2008; Garcia-Elias et al., 2008). In neurons there is also growing evidence for the concept of signaling micro-domains between channels on the cell surface and intracellular stores (reviewed by (Delmas and Brown, 2002)). More specifically, it was shown in sensory neurons that coupling of the chloride channel ANO1 to the InsP_3R enables fine-tuned signaling by this channel (Jin et al., 2013).

In the present study we used cultured primary rat dorsal root ganglia neurons (DRGN) to examine the distribution of intracellular Ca^{2+} stores and Ca^{2+} release channels in the ER, as well as the interplay between Ca^{2+} release channels in the ER with Ca^{2+} -permeable channels in the plasma membrane. We then tested whether pharmacological interference with TRPV4 signaling can modify PTX-induced neurotoxicity. In a last step, we assessed the efficacy of preventive TRPV4 inhibition in a mouse model of paclitaxel-induced neuropathy.

2. Methods

2.1. Reagents

Cremophor EL, clozapine-N-oxide, ethanol, GSK1016790A, and PTX were obtained from Sigma (St Louis, MO, USA). HC067047, ionomycin free acid, UNC3230 and xestospongine C were purchased from Tocris Bioscience (Bristol, UK). Further suppliers are mentioned where appropriate.

2.2. Lentivirus construction and production

Third-generation lentiviral particles were generated as described previously (Datwyler et al., 2011) with the following modification: pFUGW lentiviral transfer plasmid (addgene plasmid 14883, provided by Dr. David Baltimore, Lois et al. (Science. 2002 Feb 1. 295(5556):868–72.)) was modified to report exogenous expression via mCherry instead of EGFP. In a second step, a PCR fragment of hM3D DREADD (kindly provided by Dr. Bryan L. Roth (Rogan and Roth, 2011)) was inserted via BamHI-BlnI by unidirectional cloning into the parental modified lentiviral transfer plasmids expressing monomeric Cherry as a fusion to the C-terminus of the DREADD. The following primers were used to generate the PCR product (1796 base pairs of length) comprising hM3D without a stop codon: BamHI (underlined) forward primer: 5'-GCATAGGATCCATGACCTTGACACAATAACAGTAC-3' and BlnI (underlined) reverse primer: 5'-GGCTATGCTTAGCCC CAAGGCCTGCTCGGGTGC-3'. All constructs were fully sequenced prior to lentiviral particle production. Lentiviral transfer plasmids were co-transfected with packaging plasmids psPAX2 (addgene plasmid 12260) and pMD2.G (addgene plasmid: 12259, both provided by Dr. Didier Trono) into 293TN cells (BioCat, Heidelberg, Germany) using XtremeGene HP (Roche, Grenzach-Wyhlen, Germany) in OptiMEM (Gibco, Life Technologies, Karlsruhe, Germany). Two harvests of supernatant containing viral particles from the 293TN culture medium were collected 48 and 72 h after transfection. The supernatant was centrifuged at $1790 \times g$ for 15 min and filtered through a $0.45 \mu\text{m}$ low protein binding PVDF membrane (Millipore, Schwalbach, Germany). The viral particles were concentrated using 3K molecular weight cut-off concentrators (Amicon Ultra Centrifugal Filters with 3K, Millipore, Schwalbach, Germany) with $2380 \times g$ at 4°C for 30 min and by ultracentrifugation for 2 h at 4°C (Optima MAX-XP, Tabletop Ultracentrifuge with TLA-55 rotor and 43,000 rpm, that is $113,700 \times g$, Beckman Coulter, Krefeld, Germany), resuspended and aliquoted in PBS and stored at -80°C for later use. Viral transduction efficiency was determined from serial dilutions in primary neuronal cultures using mCherry fluorescence as a reporter 48 h after transduction. Viral particles were applied at a multiplicity of infection of approximately 20 with transduction units of $10^9/\text{ml}$ after concentration of lentiviral particles.

2.3. Cell culture

2.3.1. Enriched DRGN culture and transduction

All experimental procedures conformed to institutional guidelines and were approved by the State Office of Health and Social Affairs in Berlin (Landesamt für Gesundheit und Soziales (LaGeSo), Berlin, Germany). DRGN isolated from Wistar rat neonates (P1-3) were digested in 0.28 Wunsch unit collagenase (Liberase DL, Roche, Mannheim, Germany) and separated by gentle trituration. Triturated cells were passed through a $70 \mu\text{m}$ cell strainer to remove cell clumps, followed by a DRGN enrichment step via Percoll gradient centrifugation (1.019/1.038 g/ml) at $1000 \times g$ for 10 min. DRGN were plated on poly-L-lysine/laminin coated surfaces and maintained as described previously (Boehmerle et al., 2007). Cells were used in experiments 72 h after virus transduction.

2.4. Live cell imaging

2.4.1. Fura-2

Imaging experiments with Fura-2/AM were performed as described previously (Boehmerle and Endres, 2011; Boehmerle et al., 2007). In brief: Imaging was performed in HEPES buffer (in mM): 130 NaCl, 4.7 KCl, 1 MgSO_4 , 1.2 KH_2PO_4 , 1.3 CaCl_2 , 20 HEPES, 5 glucose, pH 7.4. We calculated intracellular free Ca^{2+} concentration ($[\text{Ca}^{2+}]_{\text{int}}$) from background subtracted F340/F380 fluorescence ratios (R) following in situ calibration (Grynkiewicz et al., 1985; Kao, 1994) with the following equation: $[\text{Ca}^{2+}]_{\text{int}} \text{ (nM)} = K_d * Q * (R - R_{\text{min}}) / (R_{\text{max}} - R)$. K_d is the

dissociation constant of Fura-2 for Ca^{2+} at room temperature (225 nM); Q is the fluorescence ratio of the emission intensity excited by 380 nm in the absence of Ca^{2+} to that during the presence of saturating Ca^{2+} ; R_{\min} and R_{\max} are the minimal or maximal fluorescence ratios respectively. R_{\min} was measured in Ca^{2+} free HEPES buffer (10 mM EGTA instead of CaCl_2) containing 10 μM ionomycin. R_{\max} was obtained in standard solution containing 10 mM CaCl_2 and 10 μM ionomycin. Addition of 10 μM ionomycin at the end of the experiment was used as an internal control in experiments with bath applied substances. Cells that did not respond to ionomycin stimulation (≥ 160 nM increase of $\text{Ca}_{\text{int}}^{2+}$) were excluded from evaluation. DRGN cultured in flow chambers were used for perfusion experiments. In this experiment cells were classified as TRPV4 positive if $\text{Ca}_{\text{int}}^{2+}$ increased by > 160 nM after stimulation with the agonist GSK1016790A. To identify TRPV4 immunoreactive neurons, in the presence of the inhibitor HC067047, stage coordinates of the respective experiments were saved and TRPV4 was detected with immunocytochemistry as described below. Cells were counted as TRPV4 immunoreactive if mean fluorescence was more than double background fluorescence.

2.4.2. Fluo-4

DRGN cultured on Ibidi μ -Slides (Ibidi GmbH, Martinsried, Germany) with 8 wells were incubated for 30 min at 37 °C in HEPES buffer (as described above) containing 5 μM Fluo-4/AM together with 0.02% Pluronic F-127 (both LifeTechnologies, Darmstadt, Germany). Cells were visualized on an inverted Leica TCS SP5 confocal microscope (Leica Wetzlar, Germany) with a hybrid detection system, equipped with a HCX PL APO x63/1.40 oil immersion objective. Images were acquired at 6.8 Hz. All drugs were bath applied.

2.4.3. Visualization of cell organelles

DRGN cultured on Ibidi μ -Slides (Ibidi GmbH, Martinsried, Germany) with 8 wells were incubated for 30 min at 37 °C in HEPES medium containing 500 nM ER-Tracker green to stain endoplasmic reticulum (LifeTechnologies, Darmstadt, Germany). Microscopy was performed on an inverted Leica TCS SP5 confocal microscope (Leica Wetzlar, Germany) with a hybrid detection system equipped with a HCX PL APO x63/1.40 oil immersion objective.

2.5. Cell viability assays

2.5.1. CytoTox-Fluor cytotoxicity assay

This assay measures a distinct protease activity associated with cytotoxicity (Promega, Mannheim, Germany). It was performed as described previously (Boehmerle and Endres, 2011).

2.5.2. MTT assay

Metabolic integrity of cells was assessed using MTT as described previously (Boehmerle and Endres, 2011). The MTT assay correlates with the number of live cells whereas the Cytotox-Fluor assay correlates with the number of dead cells. In order to increase sensitivity both assays were combined: background-subtracted MTT absorbance values were divided by background subtracted values of the cytotoxicity assay to obtain a live/dead ratio before normalization to control.

2.6. Histology

2.6.1. Immunocytochemistry of DRGN

DRGN were cultivated on poly-L-lysine and laminin coated coverslips. After fixation with 2% paraformaldehyde in phosphate buffered saline (PBS), cells were permeabilized with 0.1% Triton X-100. Unspecific binding sites were blocked with 10% normal goat serum (NGS) and proteins of interest identified with a primary antibody diluted in 10% NGS at 4 °C overnight. In each experiment a negative control without primary antibody was included. Primary antibodies were detected with a fluorophore-coupled secondary antibody and

mounted with ProLong Gold antifade reagent with DAPI (LifeTechnologies, Darmstadt, Germany). Antibodies used were as follows: Primary antibodies: anti-InsP₃R1 (Johanning et al., 2002); anti-InsP₃R3 (BD Biosciences Cat# 610313 RRID:AB_397705, Heidelberg, Germany); anti-RYR3 (Abcam Cat# ab77704 RRID:AB_1566702, Cambridge, UK); anti-TRPV4 (LifeSpan Cat# LS-C94498-100 RRID:AB_1941440, Seattle, OR, USA). Validation of primary antibodies was reported previously for anti-InsP₃R1 (Johanning et al., 2002), anti-TRPV4 (Ryskamp et al., 2011) and anti-InsP₃R3 (Pin et al., 2001) antibodies. Given the importance for the present manuscript, the batches of anti-TRPV4 and anti-InsP₃R1 antibodies used in this manuscript were additionally validated by western blot analysis (performed as described previously (Schlecker et al., 2006)): separation of DRGN lysate but not liver lysate showed a strong band above 100 kDa for the TRPV4 antibody used and separation of mouse cerebellar lysate but not liver lysate showed a strong band above 260 kDa for the InsP₃R1 antibody used. Secondary antibodies: goat anti-mouse IgG-Alexa 488; goat anti-rabbit IgG-QDot 625 and goat anti-rabbit IgG-Alexa 488 (all: LifeTechnologies, Darmstadt, Germany). DAPI and Qnuclear Deep Red Stain (LifeTechnologies, Darmstadt, Germany) were used to stain DNA. In addition, anti-TRPV4 was directly labeled with an Alexa-488 antibody labeling kit (A20181, LifeTechnologies, Darmstadt, Germany) and anti-InsP₃R1 with Alexa-532 according to the manufacturers protocol. Directly labeled primary antibodies were used without secondary antibody.

2.6.2. Immunohistochemistry

Specimens from adult mice, represented in Fig. 1D, were obtained from 9 week old adult C57BL/6J mice killed for cell culture purposes. Procedures conformed to animal welfare guidelines and were previously approved by the State Office of Health and Social Affairs in Berlin (LaGeSo, Berlin, Germany). Dorsal root ganglia were dissected from adult C57BL/6J mice immediately after decapitation, fixed in 4% paraformaldehyde in phosphate buffer (0.2 M NaH_2PO_4 , 0.2 M Na_2HPO_4 in distilled water, pH 7.4) and stored at 4 °C. Paraffin embedding, sectioning and staining was performed as described previously (Boehmerle et al., 2014b). In each experiment a negative control without primary antibody was included. Primary antibodies were detected with a fluorophore-coupled secondary antibody and mounted with ProLong Gold antifade reagent with DAPI (Life Technologies, Darmstadt, Germany). Primary and secondary antibodies were the same as above (Immunocytochemistry).

2.6.3. Proximity ligation assay

Proximity ligation assay reagents were purchased from Sigma-Aldrich (Taufkirchen, Germany). The assay was performed in the same permeabilized cultured DRGN as described above after labelling TRPV4 antibodies (LifeSpan Cat# LS-C94498-100 RRID:AB_1941440, Seattle, OR, USA) with plus strand (Product#: DUO92009) and InsP₃R1 (as described above) with minus strand (Product#: DUO92010). Primary antibodies were incubated at 4 °C overnight and ligation as well as amplification and detection was performed with green detection reagents (Product#: DUO92014). Samples were visualized with the same instrument as described above (Immunocytochemistry). For negative controls, only one labeled antibody was included in the reaction (Supplemental fig. 1).

2.7. Co-immunoprecipitation analysis

DRGN lysates were made by homogenization of whole dorsal root ganglia dissected from neonatal wistar rats as described above in lysis buffer (25 mM Tris-HCl pH 7.4, 150 mM NaCl, 1% NP40, 1 mM EDTA, 5% glycerol, 1x Complete protease inhibitor (Roche, Mannheim, Germany)), followed by 2 spins at 36,000 g for 5 min at 4 °C. For immunoprecipitation, the lysate was incubated with antibody in the presence of 9 mM Ca^{2+} ; the 2 antibodies used were anti-TRPV4 (#LS-

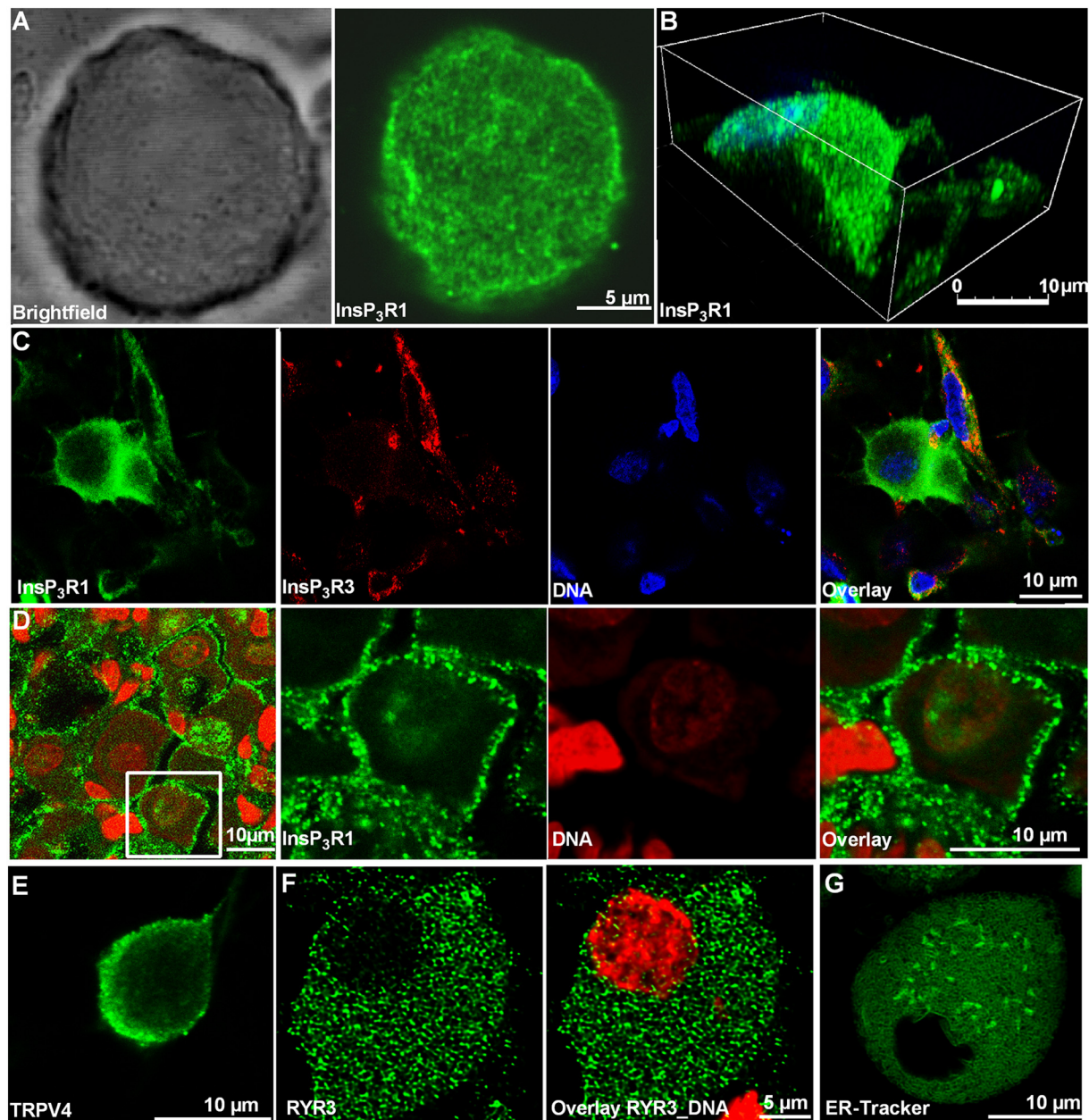


Fig. 1. Intracellular localization of Ca^{2+} channels and Ca^{2+} stores in DRGN.

Cultured DRGN from postnatal rats express high levels of InsP_3R type 1. (A) Tangential section through the cell: The InsP_3R type 1 shows a reticular pattern of immunoreactivity. (B) The volume model generated from serial z sections of a rat DRGN stained for InsP_3R type 1 (green) and DNA (blue) shows InsP_3R type 1 immunoreactivity concentrated in the cells periphery. (C) Analysis of InsP_3R subtypes shows that InsP_3R type 1 (green) is mainly observed in rat DRGN and to a lesser extend in glia; the latter mostly expresses InsP_3R type 3 (red). (D) Similar InsP_3R distribution patterns were also observed in tissue from adult mice: a peripheral pattern of InsP_3R distribution could also be observed in paraffin sections of lumbar dorsal root ganglia from C57BL/6 mice (left: overview, white box indicates area magnified in the panels to the right). (E) Staining of TRPV4 in cultured DRGN showed a distribution typical for a channel located in the plasma membrane. (F) In contrast to the peripheral localization of the InsP_3R type 1, the ryanodine receptor type 3 could be detected in a similar pattern compared to (G) the ER (ER Tracker green). (For interpretation of the references to colour in this figure legend, the reader is referred to the web version of this article.)

C94498, LifeSpan BioSciences, Seattle, OR, USA) and anti- InsP_3R 1 (Johanning et al., 2002). Immunoblotting for InsP_3R 1 and TRPV4 was performed as described previously (Boehmerle and Endres, 2011) with the same samples loaded on two gels.

performed with Amira 6 (FEI Visualization Sciences Group, Burlington, MA, USA) while ImageJ software (National Institutes of Health, Bethesda, MD) (Schindelin et al., 2012) was used to calculate $\Delta F/F_0$, analyze mean fluorescence intensity values, perform co-localization analysis and to overlay images for publication.

2.7.1. Image acquisition and analysis

Specimens were visualized on a Leica TCS SPE or Leica TCS SP5 confocal microscope (Leica Wetzlar, Germany). Obtained image stacks were deconvolved with Huygens Essential (Scientific Volume Imaging b.v., Hilversum, The Netherlands) and 3D reconstructions were

2.8. In vivo

2.8.1. Animal numbers, housing and methods of randomization and blinding

A total of 40 male 9-week old C57BL/6 mice from Charles River (Sulzfeld, Germany) were used in this experiment. All experimental procedures conformed to animal welfare guidelines and were previously approved by the State Office of Health and Social Affairs in Berlin (LaGeSo, Berlin, Germany). Upon arrival, mice were randomized with the help of an online randomization tool (GraphPad Software, La Jolla, CA, USA; <https://www.graphpad.com/quickcalcs/randomize1.cfm>) to four different treatment groups: Mice received either four intraperitoneal injections of 1 mg/kg bodyweight paclitaxel (PTX) every other day (day 0, 2, 4, 6) or the corresponding vehicle (VEH; Cremophor EL:ethanol 1:1). In addition, mice were either injected intraperitoneally with the TRPV4 inhibitor HC067047 (10 mg/kg bodyweight) or the corresponding vehicle (DMSO) prior to every PTX or VEH injection. Sample sizes of this 2-variable four group experiment (VEH/VEH, PTX/VEH, VEH/HC, PTX/HC) were determined prior to the experiment using G*Power open-source software (Faul et al., 2009) based on previously observed effect sizes in electrophysiological outcome parameters (Boehmerle et al., 2014a) with a desired power of 0.8 and an alpha-error of 0.05 based on an intended 2-way ANOVA statistical analysis. All investigators involved with the behavior and electrophysiological experiments were blinded throughout the entire process.

2.8.2. Drug application

Paclitaxel was dissolved in Cremophor EL:ethanol 1:1 to a concentration of 6 mg/ml (stock solution) and diluted in sterile 0.9% saline solution to a final concentration of 0.1 mg/ml. Cremophor EL:ethanol 1:1 was likewise diluted in 0.9% saline solution to a final concentration of 1:60. HC067047 was dissolved in DMSO to a concentration of 10 mg/ml and diluted to a final concentration of 1 mg/ml in sterile 0.9% saline solution and injected prior to every PTX or VEH injection. As vehicle treatment, DMSO was diluted to a final concentration of 1:10 in sterile 0.9% saline solution and injected prior to every PTX or VEH injection in the VEH/VEH and PTX/VEH groups. All substances were applied intraperitoneally at 10 μ l/g bodyweight. The general well-being of the mice was checked daily and their weight recorded.

2.8.3. Behavior analysis and nerve conduction studies

Mice were familiarized to the blinded investigator on five consecutive days prior to the experiment. For behavior analysis, cages and animals were randomly selected and testing was carried out in a dedicated laboratory with soundproof chambers between 10 am and 4 pm. Mice were trained in the Rotarod test to determine locomotor function as previously described (Boehmerle et al., 2014b). The latency to fall off the rod was measured automatically by a floor sensor (TSE Systems, Bad Homburg, Germany). Assessment of the mechanical withdrawal threshold was obtained with an electronic von Frey device (Boehmerle et al., 2014b): after placing the mice individually in a clear inverted plastic cage with a wire-mesh floor, a hand-held force transducer (IITC, Woodland Hills, CA, USA) was fitted with a 0.5 mm² semiflexible polypropylene tip and increasing pressure to the center of the hind paws was applied by a trained investigator over 5 s until it evoked a clear withdrawal response of the paw. The mechanical withdrawal threshold in grams (g) was measured automatically by the device. The maximum applied force was 10 g (Huehnchen et al., 2013). Sensory nerve action potential (SNAP) were recorded from the tail nerve in inhalation anesthesia (1.5% isoflurane/50% O₂) with a customized Neurosoft Evidence 3102evo ENG device (Schreiber & Tholen Medizintechnik GmbH, Stade, Germany) as described previously (Boehmerle et al., 2014a). In brief: stimulating needle electrodes were positioned at the base of the tail with the recording electrodes placed approx. 5 cm distal. Stimulation intensity was gradually increased

manually to supramaximal level and afterwards 100 consecutive supramaximal stimuli of 0.1 ms each were applied and averaged to obtain SNAP amplitudes and nerve conduction velocity (NCV).

2.9. Data and statistical analysis

The manuscript was prepared according to ARRIVE guidelines (Kilkenny et al., 2010). Data are expressed as mean \pm SEM or as representative traces. (n/N) describes the number of cells studied (n) in (N) independent cultures. Statistical outliers that met Peirce's criterion were excluded (Dardis, 2004; Ross, 2003). Prism v6.0 (GraphPad Software, La Jolla, CA, USA) was used for data visualization and statistical analysis. Data was checked for Gaussian distribution prior to statistical analysis using Shapiro-Wilk normality test. If distribution was normal, statistical analysis of the differences between treated versus control groups was performed by using a one- or two-way ANOVA with the Holm-Sidak post hoc test. Dunn's method was used for samples which failed the normality test. If 2 groups were compared, normally distributed data was analyzed using unpaired two-sided *t*-tests and not normally distributed data was analyzed with Mann-Whitney-U Test. *p* < 0.05 was considered statistically significant.

3. Results

3.1. Localization of intracellular Ca²⁺ stores and Ca²⁺ release channels in DRGN

Given the high relevance of a tightly regulated intracellular Ca²⁺ homeostasis we were interested in the localization of Ca²⁺ stores and Ca²⁺ release channels in DRGN. As a first step, we studied InsP₃R1 localization in cultured small to medium size (< 45 μ m) rat DRGN, as previous studies suggested a functional relevance of this InsP₃R subtype in sensory neurons (Jin et al., 2013) and we previously demonstrated altered InsP₃ mediated Ca²⁺ signals in paclitaxel treated DRGN (Boehmerle et al., 2007). We observed InsP₃R1 immunostaining in a reticular pattern typical for a protein located in the ER and with a strong signal in the periphery of cells (Fig. 1A). Three dimensional reconstruction of serial z sections obtained with confocal microscopy confirmed a predominant peripheral localization of InsP₃R1 (Fig. 1B, Supplemental Figs. 2–3). The type of distribution depicted in Fig. 1B with very strong immunoreactivity close to the plasma membrane was observed in 35 \pm 4% of cells (37/6, *p* < 0.05). An additional 19 \pm 3% of cells showed a mixed pattern with strong immunoreactivity in the periphery, but also a reticular pattern in the cytoplasm and 46 \pm 4% of cells showed a more uniform distribution of InsP₃R1. It was previously reported, that the InsP₃R type 3 constitutes > 50% of InsP₃Rs in the Neuro-2a neuroblastoma cell line (De Smedt et al., 1997). We therefore analyzed in a next step staining for type 1 and type 3 InsP₃R in cultured rat dorsal root ganglia. We observed virtually no InsP₃R type 3 signal in DRGN (round cell in the center of the image Fig. 1C) but high expression levels in cells showing morphological features of a contaminating Schwann cell (elongated cell in Fig. 1C). To exclude the possibility that the observed InsP₃R1 distribution was an artifact of cell culture, species dependent or restricted to the postnatal period, we repeated this experiment in paraffin sections of lumbar dorsal root ganglia dissected from adult C57BL/6 mice. We observed the same staining pattern as in cultured DRGN (Fig. 1D), which is similar to channels in the plasma membrane such as TRPV4 (Fig. 1E). Another family of Ca²⁺ release channels located in the ER are ryanodine receptors (RyR). In the brain and sensory neurons, the most common isoform is RyR3 (Ouyang et al., 2005). RyR3 immunofluorescence in cultured DRGN was detected throughout the cytoplasm in a reticular pattern (Fig. 1F). This pattern corresponds to the distribution of the ER which was visualized with ER tracker green, a fluorescence labeled form of glibenclamide. Glibenclamide binds to the sulphonylurea receptors of ATP-sensitive K⁺ channels which are

prominent on the ER and the fluorophore-bound derivative of glibenclamide allows visualization of the ER in live cells. In the resulting live-cell staining, the ER was distributed in a reticular pattern throughout the cytoplasm (Fig. 1G). In summary, we could show that InsP₃R1 but not InsP₃R3 is highly expressed in small to medium size DRGN and that InsP₃R1 is frequently concentrated in the periphery of DRGN. This finding is in contrast to the distribution of RYR3 and the ER, observed in the same cell type.

3.1.1. Spatial distribution of InsP₃ mediated Ca²⁺ signals in DRGN

We hypothesized that the peripheral distribution of InsP₃R1 may enable the formation of signaling domains with Ca²⁺ channels in the plasma membrane, as was observed for Ca²⁺ dependent chloride channels (Jin et al., 2013). However, the assessment of InsP₃-mediated Ca²⁺ signals in the presence of extracellular Ca²⁺ is challenging, as many agonists of metabotropic receptors such as the purinergic P2Y receptor family also activate ionotropic receptors and receptor distribution in DRGN is often heterogeneous (Kobayashi et al., 2013). To circumvent this problem and to facilitate identification of responsive neurons, we transduced cultured DRGN with a lentivirus expressing the fluorescent protein mCherry as a C-terminal fusion to a designer receptor exclusively activated by a designer drug (DREADD) derived from the metabotropic M₃ muscarinic acetylcholine receptor (Armbruster et al., 2007). The hM₃D DREADD responds to clozapine-N-oxide (CNO). CNO stimulation leads to the G_q mediated activation of phospholipase C and formation of InsP₃. The advantage of this approach is that cells which are responsive to the agonist can be clearly identified by red mCherry fluorescence. DRGN expressing the hM₃D receptor were loaded with the non-ratiometric fluorescent Ca²⁺ indicator Fluo-4, and the spatial response was studied with confocal microscopy. Adding the agonist CNO led to a rapid increase of cytoplasmic Ca²⁺ (Fig. 2A) with a strong increase of fluorescence close to the plasma membrane as would be expected by the distribution of InsP₃Rs (Fig. 2B).

We further characterized the Ca²⁺ signals induced by CNO stimulation in hM₃D-expressing DRGN loaded with the ratiometric Ca²⁺ indicator Fura-2. Application of 10 μM CNO led to a mean increase of 162 nM ± 2 nM Ca²⁺_{int} (79/6) in Ca²⁺ containing and 101 nM ± 2 nM Ca²⁺_{int} (58/5) in Ca²⁺-free buffer. Untransduced cells did not respond to CNO stimulation with a mean change in Ca²⁺_{int} of 5.0 nM ± 0.1 nM (85/6) (p < 0.001 compared to transduced cells; Fig. 2C). Application of vehicle likewise had no effect on hM₃D-expressing cells, with a mean change in Ca²⁺_{int} of 1.0 nM ± 0.1 nM (59/5; p < 0.001; Fig. 2D-E). In order to confirm that the Ca²⁺ signal observed is initiated via InsP₃Rs, phospholipase C and the InsP₃R were blocked in the presence of extracellular Ca²⁺. Inhibition of phospholipase C with 10 μM U73122 almost completely abrogated the response, with an average Ca²⁺_{int} increase of 32 nM ± 1 nM (45/6; p < 0.001 compared to CNO alone; not significant compared to vehicle; Fig. 2D-E). InsP₃R were blocked with 5 μM xestospongine C, which led to a similar effect: Ca²⁺_{int} after stimulation with CNO was only 29 nM ± 1 nM (66/5, p < 0.001 compared to CNO alone; not significant compared to vehicle; Fig. 2D-E). These results confirm that stimulation of hM₃D transduced cells with CNO leads to a phospholipase C and InsP₃R-generated Ca²⁺ signal, which corresponds to histological InsP₃R1 localization.

3.1.2. Interaction of InsP₃R and TRPV4 channels

Previous reports found that TRPV4 functionally interacts with InsP₃R3 in epithelial cells (Fernandes et al., 2008; Garcia-Elias et al., 2008). We hypothesized that in sensory neurons TRPV4 may interact with InsP₃R1, with potential implications for the pathogenesis of PTX-induced neurotoxicity (Alessandri-Haber et al., 2004; Boehmerle et al., 2006). Our observation that DRGNs stimulated with CNO in the presence of extracellular Ca²⁺ showed a considerably higher response compared to experiments performed under Ca²⁺ free conditions (Fig. 2) also suggests a potential functional interaction. To test this hypothesis, we quantified the response to CNO stimulation in TRPV4 positive hM₃D

transduced cells by first perfusing cells with CNO, followed by a brief wash out phase and subsequent stimulation of TRPV4 channels with the highly selective TRPV4 agonist GSK1016790A. The average InsP₃-mediated increase in Ca²⁺_{int} in the presence of extracellular Ca²⁺ of TRPV4⁺ cells with this paradigm was 250 nM ± 5 nM (25/5; Fig. 3A+C). To assess the contribution of TRPV4 mediated Ca²⁺ entry, TRPV4 channels were blocked with the selective antagonist HC067047. To achieve a near maximal blockade a dose of 2 μM HC067047 (approx. 15 times IC₅₀ (Everaerts et al., 2010)) was bath applied immediately before the experiment. As stimulation of TRPV4⁺ cells with GSK1016790A after blockade of TRPV4 with HC067047 proved to be difficult, TRPV4⁺ cells were identified by immunocytochemistry subsequent to Ca²⁺ imaging. In the presence of HC067047 the average increase of Ca²⁺ in TRPV4⁺ cells was 102 nM ± 2 nM (39/6; p < 0.001 compared to TRPV4⁺; Fig. 3B-C). These observations lend support to the concept that Ca²⁺-signaling between the InsP₃R and the Ca²⁺ permeable cation channel TRPV4 is able to modulate intracellular Ca²⁺ signals in TRPV4 expressing DRGN. To further assess the InsP₃R1-TRPV4 interaction, we performed a costaining of these receptors with directly labeled antibodies. Visual assessment showed partial co-localization between TRPV4 and InsP₃R1 immunoreactivity (Fig. 3D). Numerical analysis of double-labeled image stacks with the open source JACoP tool (Bolte and Cordelieres, 2006) calculated an overlap coefficient r of 0.874 and Costes' randomization based co-localization resulted in a highly significant p-value (100%, this p-value is inversely correlated to the probability of getting the specified co-localization by hazard). Analysis with the Van Steensel's approach showed a shift of the peak in the cross-correlation analysis as observed in partially colocalizing structures (Bolte and Cordelieres, 2006). To test for a possible physical interaction, InsP₃R1 and TRPV4 were immunoprecipitated from dorsal root ganglia tissue lysate. Both proteins could be detected in tissue lysate (Fig. 3E) and as shown in previous publications (Arniges et al., 2006) three bands were detected for TRPV4 in native lysate. After immunoprecipitation in the presence of Ca²⁺ with either anti-TRPV4 or anti-InsP₃R1 antibody, both proteins could be detected in an immunoblot for InsP₃R1 or TRPV4, while the bead control showed no immunoreactivity (Fig. 3E). Interestingly, after pull-down with InsP₃R1 only the 96 kDa band of TRPV4 was detected, suggesting that only the non-glycosylated form of TRPV4 interacts with the InsP₃R1. This finding may explain why only partial co-localization was observed in immunocytochemistry. Next, we used a fluorescent proximity ligation assay (PLA) which is positive if two proteins are closer than approximately 30 nm (Soderberg et al., 2006). Using this assay for TRPV4 and InsP₃R1 we observed punctate fluorescent signals, which were concentrated in the periphery of DRGN (Fig. 3F), further supporting a physical interaction between TRPV4 and InsP₃R1 in small to medium size sensory neurons. No PLA signal was observed in contaminating non-neuronal cells. In summary, we could demonstrate partial co-localization as well as a close proximity and physical as well as functional interaction between the InsP₃R1 and TRPV4 channels.

3.1.3. Ca²⁺ signaling and PTX-induced toxicity

The cytostatic drug PTX induces cell death in DRGN, at least in part, through InsP₃R-mediated Ca²⁺ release from the ER and subsequent activation of the Ca²⁺-activated protease calpain (Boehmerle et al., 2007). If Ca²⁺-signaling micro-domains between the InsP₃R and the cation channel TRPV4 have functional relevance, inhibition of this channel should be neuroprotective. As a first step we established a dose-response curve for PTX-induced cytotoxicity in enriched DRGN cultures which were treated for 24 h with PTX. We chose this longer incubation period to mimic findings from human pharmacokinetic studies (Huizing et al., 1993). In contrast to our previous observations in DRGN treated with PTX for 6 h (Boehmerle et al., 2007), we observed dose dependent toxicity at this time point. The calculated EC₅₀ was 33 nM (non-linear regression fit; Fig. 4A); for further experiments we chose 100 nM as a dose which leads to a near maximal effect. The PTX dose used in our

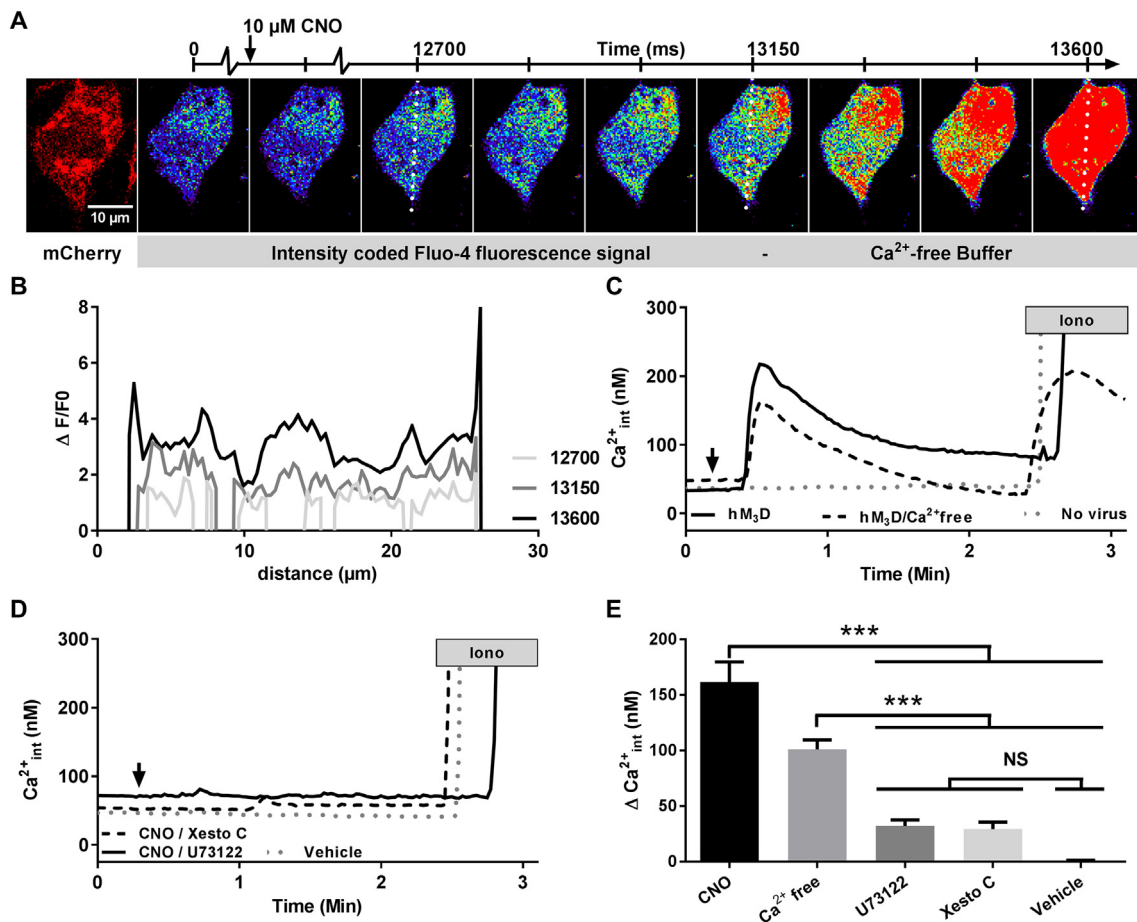


Fig. 2. Localization and characteristics of InsP_3 mediated Ca^{2+} signals in DRGN.

InsP_3 mediated Ca^{2+} signals were studied in DRGN expressing hM₃D DREADDs labeled with the fluorescent protein mCherry. (A) Time series of a DRGN transduced with hM₃D loaded with the non-ratiometric fluorescent Ca^{2+} indicator Fluo-4. Fluorescence intensity is colour coded: cool colors (blue) represent low and hot colors (red) high Ca^{2+} concentrations. (B) Line profiles of fluorescence intensity measured along the white dotted line from the cell shown in panel A: Fluorescence intensity was normalized to background fluorescence ($\Delta F/F_0$) and plotted for 3 distinct time points: In the absence of extracellular Ca^{2+} , a strong Ca^{2+} signal close to the plasma membrane can be observed, corresponding to the histological receptor distribution. To quantify Ca^{2+} signals, the ratiometric fluorescent Ca^{2+} indicator Fura-2 was used in subsequent experiments: (C) Representative Ca^{2+} response to stimulation with clozapine-N-oxide (10 μM CNO, arrow) in untransduced DRGN (grey dotted line) and hM₃D receptor expressing DRGN in Ca^{2+} containing (solid line) and Ca^{2+} -free buffer (dashed line). (D-E). Pharmacological inhibition of phospholipase C with U73122 (black solid line) or the InsP_3 R with xestospongine C (Xesto C, black dashed line) almost completely abrogates the response to CNO in hM₃D expressing cells. Treatment of hM₃D expressing cells with vehicle (DMSO) does not induce alterations of $\text{Ca}^{2+}_{\text{int}}$ (grey dotted line). *** $p < 0.001$ (One-way ANOVA with Holm-Sidak post hoc test). (For interpretation of the references to colour in this figure legend, the reader is referred to the web version of this article.)

study reflects previously published tissue levels in dorsal root ganglia of PTX treated mice (Xiao et al., 2011). In this study PTX tissue concentrations were highest in dorsal root ganglia, which suggests that primary DRGN are a relevant cell model for the examination of molecular mechanisms underlying paclitaxel-induced polyneuropathy. In a next step, DRGN were incubated with increasing concentrations of HC067047, an inhibitor of the TRPV4 channel, in the presence of PTX or vehicle. We observed that a dose of 100 nM HC067047, which is close to the IC_{50} of 133 nM (Everaerts et al., 2010), significantly reduced PTX-induced cytotoxic effects by $59\% \pm 6\%$ ($n = 6$; $p < 0.001$; Fig. 4B). Higher doses of HC067047 showed a strong trend towards toxic effects in vehicle-treated cells, which may explain why doses higher than 200 nM were not neuroprotective. Taken together, these findings support the pathophysiological relevance of TRPV4 channels in PTX-induced neurotoxicity.

3.1.4. Neuroprotective effects of TRPV4 inhibition in paclitaxel-induced neuropathy

To test the neuroprotective capacities of TRPV4 inhibition in a more complex in vivo setting, we designed a preventive experiment: adult C57BL/6 mice were treated with the TRPV4 inhibitor HC067047

(10 mg/kg bodyweight) or vehicle prior to every paclitaxel or vehicle injection and animals were repeatedly tested for the development of sensory neuropathy (Fig. 5A). We had previously shown that four injections of 1 mg/kg bodyweight paclitaxel over the course of 6 days leads to the development of a sensory axonal neuropathy without affecting the general well-being of the mice or their locomotor function (Boehmerle et al., 2014a). Application of HC067047 in combination with PTX did not result in general side effects as all mice showed a similar weight gain (Fig. 5B). One animal in the PTX/HC067047 group died during intraperitoneal injection. Locomotor function assessed with the rotarod test was neither affected by PTX or HC067047 application (Fig. 5C). In line with our previous results, we observed a significant decrease in the mechanical withdrawal threshold in PTX/VEH treated mice indicative of mechanical allodynia, whereas PTX treated mice which also received HC067047 were protected from these changes ($n = 10/\text{group}$, $p = 0.0278$, Fig. 5D). More importantly, neurographic measurements of sensory fibers showed that HC067047 treated mice did not develop the decrease of SNAP amplitude which occurs after PTX application alone ($n = 10/\text{group}$, $p = 0.0033$, Fig. 5E+F). Taken together, these results indicate that in the context of PTX-induced neuropathy, preemptive inhibition of TRPV4 is neuroprotective.

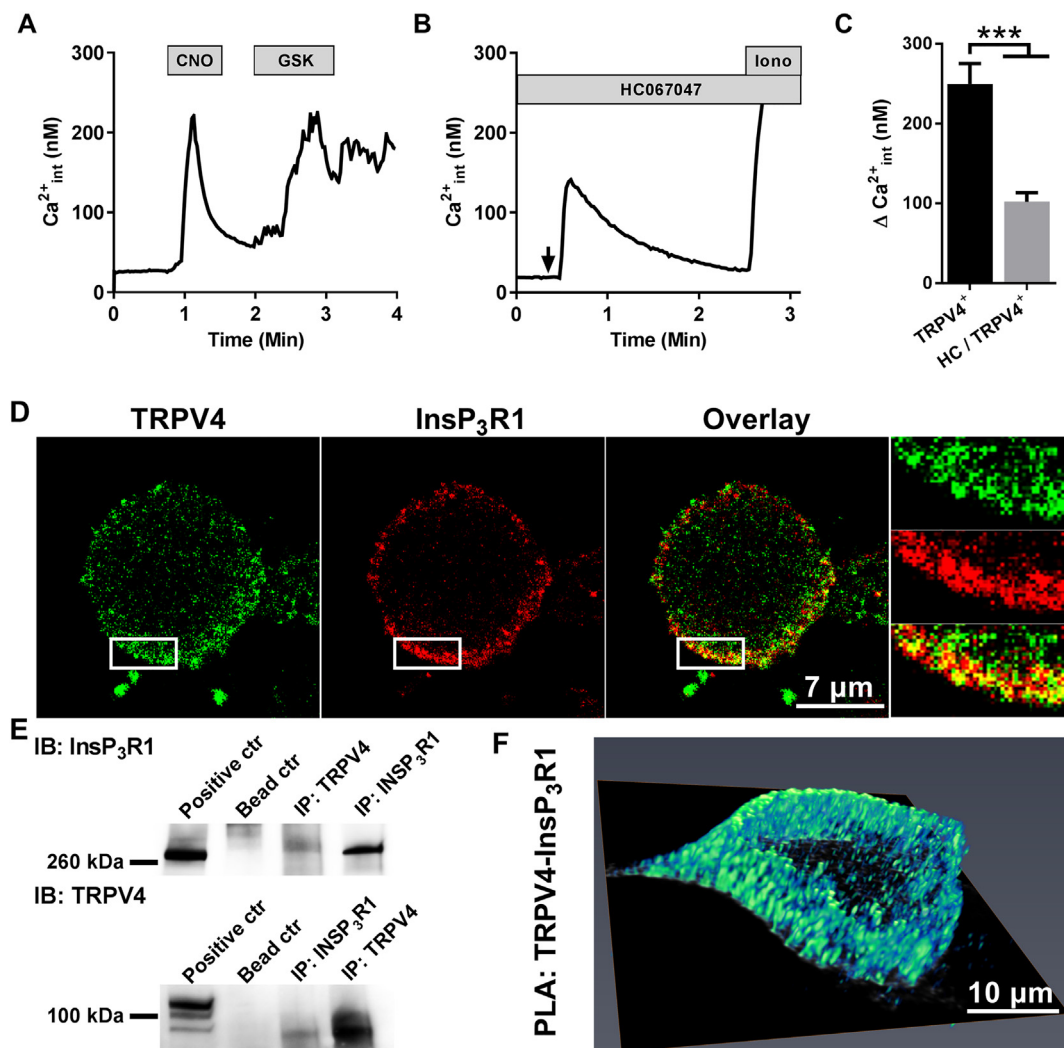


Fig. 3. Interaction analysis of TRPV4 and InsP₃R1.

(A) InsP₃ mediated Ca²⁺ signals in TRPV4 positive neurons in DRGN expressing hM₃D DREADDs were measured by sequential stimulation with CNO and the TRPV4 agonist GSK1016790A. (B)–(C) Pharmacological inhibition of TRPV4 channels with HC067047 (HC) leads to significantly smaller InsP₃ induced Ca²⁺ signals in TRPV4 immunoreactive neurons. (D) Representative costaining of InsP₃R1 and TRPV4, detected with primary labeled antibodies. Visual assessment shows partial colocalization between TRPV4 and InsP₃R1 immunoreactivity (stacked rectangles on the right side present a zoomed view of the insets in each panel). (E) Co-immunoprecipitation of TRPV4 and InsP₃R: Lanes with positive control were loaded with DRGN tissue lysate; lanes with bead control were loaded with beads treated with rabbit pre-immune serum; immunoprecipitation (IP) was performed with anti-TRPV4 respectively anti-InsP₃R1 antibody. Upper panel shows an immunoblot (IB) for InsP₃R1 and lower panel an immunoblot for TRPV4. Three bands were detected for TRPV4 in native lysate (lane1), after pull-down with InsP₃R1 only the 96 kDa band of TRPV4 was detected, suggesting that only the non-glycosylated form of TRPV4 interacts with the InsP₃R1. (F) Interaction of TRPV4 and InsP₃R1 in cultured DRGN was further studied with a fluorescent proximity ligation assay (PLA) which is positive if two proteins are closer than approximately 30 nm. The image shows a pseudocolored (blue to yellow; yellow represents higher fluorescence intensities) 3 dimensional reconstruction of serial z-sections through a DRGN with punctate fluorescent signals located in the cells periphery. ***p < 0.001 (C: Mann-Whitney-U Test). (For interpretation of the references to colour in this figure legend, the reader is referred to the web version of this article.)

4. Discussion

Ca²⁺ is an important and versatile intracellular messenger which is involved in the regulation of many cellular functions, among others, cell survival, neurotransmitter release, synaptic plasticity but also cell death (reviewed by (Berridge, 1998; Berridge et al., 1998)). Regulation of completely dissimilar cellular processes through the same second messenger is enabled by fine-tuned modulation of the spatial and temporal pattern of Ca²⁺ signals. The existence of a large “Ca²⁺-signaling toolkit” has been suggested for that purpose (Berridge et al., 2003), but its composition in peripheral neurons and alterations in the pathogenesis of neuropathies are still a matter of research. The aim of the present study was to further characterize this “Ca²⁺ toolkit” in small to medium size primary sensory neurons in the context of

paclitaxel-induced neurotoxicity. We observed that in DRGN the ER was distributed throughout the cytoplasm. In contrast to the homogenous ER distribution, InsP₃R type 1 was typically concentrated in the periphery of DRGN. Further examination of intracellular Ca²⁺ release channels revealed that InsP₃R type 3 was only observed in cells showing morphological features of contaminating glia, but not in DRGN and that RYR did not show the specialized distribution of InsP₃Rs. Given the considerable heterogeneity of G-protein coupled receptors in DRGN, we used DREADDs to further elucidate InsP₃-mediated Ca²⁺ signals and to minimize interference with other receptors (Armbruster et al., 2007). Specifically, a DREADD derived from the muscarinic M₃ receptor which activates G_{q/11} and subsequently phospholipase C was used to characterize phosphoinositide-mediated Ca²⁺ signaling. This approach showed InsP₃-mediated Ca²⁺ signals close to the plasma membrane as

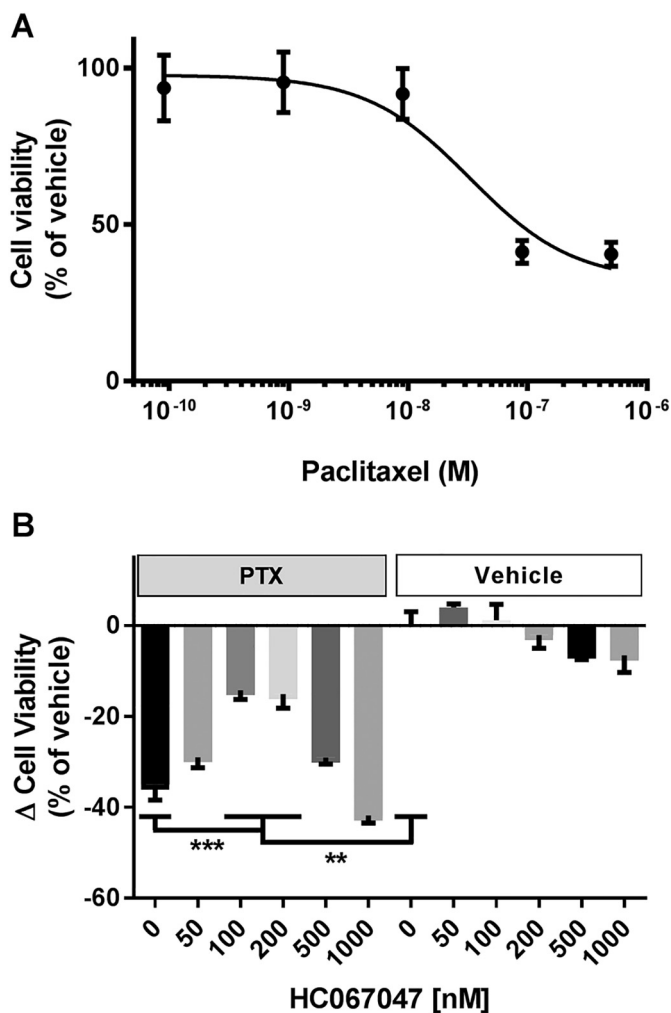


Fig. 4. PTX-induced cytotoxicity in cultured DRGN.

(A) Dose-response curve of PTX-induced cytotoxicity after 24 h PTX exposure in cultures enriched for rat postnatal DRGN. Data was fitted with a three parameter logistic curve. (B) Toxicity induced by incubation of DRGN with 100 nM PTX for 24 h can be ameliorated by pharmacological inhibition of TRPV4 channels with the compound HC067047 (left side of the graph “PTX”). Incubation with the solvent of PTX (right side of the graph “Vehicle”) with increasing concentrations of HC067047 for 24 h showed a trend towards toxic effects of higher doses HC067047. ***p* < 0.01; ****p* < 0.001 (B: One-way ANOVA with Holm-Sidak post hoc test)

would be expected by InsP₃R distribution. We found that in the presence of extracellular Ca²⁺, InsP₃-induced Ca²⁺ transients were amplified by Ca²⁺ entry through the plasma membrane and that the TRPV4 channel contributes to this Ca²⁺ signal in TRPV4 expressing sensory neurons. Co-labeling, co-immunoprecipitation and proximity ligation assay experiments showed partial co-localization as well as a physical interaction between the InsP₃R1 and the non-glycosylated form of TRPV4. This is an interesting observation, as the non-glycosylated form of TRPV4 was shown to mediate larger TRPV4 mediated Ca²⁺ signals in response to hypotonicity in human embryonic kidney cells (Xu et al., 2006). These results suggest the presence of Ca²⁺-signaling micro-domains between the InsP₃R and TRPV4 channels in the plasma membrane, similar to observations made in epithelial cells (Fernandes et al., 2008; Garcia-Elias et al., 2008) and for the chloride channel ANO1 with the InsP₃R1 in sensory neurons (Jin et al., 2013). These micro-domains appear to be functionally relevant as inhibition of Ca²⁺ entry through TRPV4 reduced PTX-induced-neurotoxicity. To further demonstrate the molecular interaction, the work in the present

manuscript could be expanded by using additional experimental techniques such as immuno-EM in future studies.

Different subsets of sensory neurons express various members of the TRP ion channel family which serve as molecular sensors for a number of chemical- and physical stimuli (reviewed by (Basbaum et al., 2009)). A number of TRP channels including TRPV4, TRPV1 and TRPA1 were shown to play a role in mouse and rat models of paclitaxel-induced neurotoxicity in the peripheral nervous system. These channels appear to be compulsory for the development of mechanical and thermal allodynia/hyperalgesia, as pharmacological inhibition or genetic knockout ameliorated or abrogated these paclitaxel-induced polyneuropathy symptoms (Alessandri-Haber et al., 2004; Chen et al., 2011; Costa et al., 2017; Materazzi et al., 2012). One caveat of the aforementioned studies is the focus on behavior endpoints, which do not address the question of whether TRP channels take an active part in PTX-induced neurotoxicity or whether they mainly contribute to the development of symptoms. In the context of our study, we hypothesized that TRPV4 channels contribute to the development of intracellular Ca²⁺ dyshomeostasis, as intracellular Ca²⁺ levels play an important role in the regulation of many TRP channels (Clapham, 2003). Previously, it was shown that an increase in intracellular Ca²⁺ potentiates TRPV4 currents at low resting Ca²⁺ concentrations (Strotmann et al., 2003), while high levels of intracellular Ca²⁺ inhibit TRPV4 gating (Watanabe et al., 2003). These results suggest a dynamic interaction between store operated Ca²⁺ release and TRP mediated Ca²⁺ entry. In the case of TRPV4 this interplay has been observed in both directions depending on the cell type: It was shown in astrocytes that TRPV4 mediated influx of Ca²⁺ ions is amplified by Ca²⁺-induced Ca²⁺ release from the ER involving InsP₃R (Dunn et al., 2013), whereas in epithelial cells InsP₃-mediated Ca²⁺ release was shown to sensitize TRPV4 channels (Fernandes et al., 2008; Garcia-Elias et al., 2008). The highly localized distribution of InsP₃R in sensory neurons suggests that in these cells both mechanisms are of potential relevance. In the context of PTX-induced Ca²⁺ signals, binding of PTX to NCS-1 would lead to a positive modulation of the InsP₃R and an increased Ca²⁺ release from the ER (Boehmerle et al., 2006; Zhang et al., 2010). This signal is amplified by Ca²⁺ induced (positive) modulation of TRPV4 (and possibly other) channels in the plasma membrane. The resulting Ca²⁺ levels are then high enough to trigger cytotoxic signaling pathways. Although our observations suggest a sequential activation of different Ca²⁺ sources, an alternative scenario where TRP channels in the plasma membrane are directly modulated by PTX bound to NCS-1 with a resulting independent Ca²⁺ influx through both Ca²⁺ channels cannot be entirely precluded. Another caveat of the present study is that although the specificity of HC067047 for TRPV4 channels was previously verified for the concentration range used in the present manuscript (Everaerts et al., 2010), off-target effects cannot be precluded. In addition, cross talk of signaling cascades downstream of M3 activation are possible in experiments involving DREADDs. To strengthen the proposed hypothesis, the interaction site of TRPV4 and InsP₃R1 should be identified and inducible genetic approaches be used in future experiments.

In a mouse model of PTX induced sensory neuropathy TRPV4 inhibition prevented symptoms, including alterations of tail SNAP amplitude. Our results thus support the pathophysiological relevance of an altered intracellular Ca²⁺ homeostasis in PTX-induced neurotoxicity. Interestingly, TRPV4 mutations were found in patients with the hereditary Charcot Marie Tooth disease type 2C. These mutations lead to a gain of channel function, resulting in elevated baseline and stimulated Ca²⁺ levels, which are thought to contribute to neurodegeneration (Deng et al., 2010; Klein et al., 2011; Landouere et al., 2010). Similar to paclitaxel-induced polyneuropathy, nerve histology and electrophysiological evaluation of patients with Charcot Marie Tooth disease type 2C show a predominantly axonal neuropathy; however even though sensory neuropathy occurs, motor symptoms dominate the phenotype. Furthermore, an abnormal intracellular Ca²⁺ homeostasis

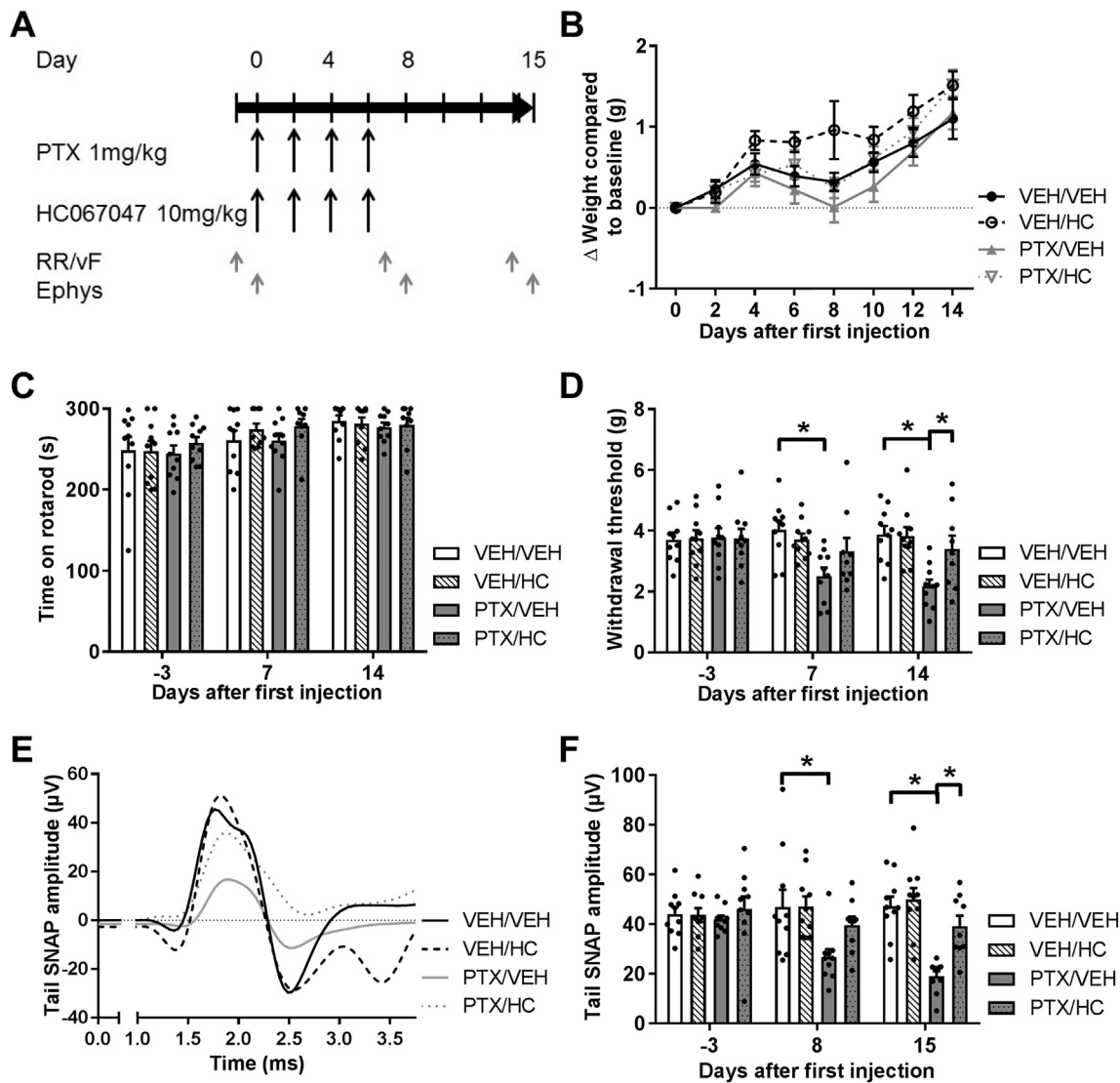


Fig. 5. Evaluation of preemptive TRPV4 inhibition in PTX-treated mice.

(A) Schedule of treatment with PTX respectively the TRPV4 inhibitor HC067047 (HC) or vehicle (VEH) and behavioral (RR Rotarod, vF von Frey Hair) as well as electrophysiological assessment (Ephys). Overall, 4 groups with 10 mice each were formed receiving PTX/VEH, PTX/HC, VEH/HC and VEH/VEH treatment. (B) Treatment was well tolerated in all groups and (C) animals showed similar performance in the Rotarod test. (D) The mechanical withdrawal threshold in the hind paws was significantly reduced in PTX/VEH treated animals compared to VEH/VEH but more importantly also compared to animals receiving PTX/HC treatment. (E) Representative sensory nerve action potential (SNAP) amplitude recordings in tail nerves from treatment groups at day 14. (F) PTX/VEH treated animals showed a significant reduction of the SNAP amplitude by approx. 50%, whereas preventive TRPV4 inhibition maintained axonal integrity during PTX therapy. * $p < 0.05$ (D + F: ordinary 2-way ANOVA with Holm-Sidak post hoc test).

has also been implied as an important early factor in diabetic neuropathy (reviewed by (Verkhatsky and Fernyhough, 2008)). The observation of Ca^{2+} dyshomeostasis in toxic, metabolic and hereditary neuropathies suggests the possibility of potentially comprehensive treatment strategies worth further exploration.

In summary, we report that in small to medium size DRGN $InsP_3R$ type 1 is typically concentrated in the cell periphery, whereas RYR3 and the ER are more evenly distributed throughout the cell. This distribution is functionally relevant, as strong $InsP_3$ -mediated Ca^{2+} signals can be observed close to the plasma membrane, which can be amplified by Ca^{2+} entry through TRPV4 channels. In addition to this functional interaction, our data supports a physical interaction of $InsP_3R1$ with TRPV4. In the pathogenesis of PTX-mediated neurotoxicity, Ca^{2+} signaling micro-domains appear to be involved, as inhibition of Ca^{2+} entry through TRPV4 channels partially prevented cell death and the development of PTX-induced neuropathy in mice. These findings provide a novel approach to understanding Ca^{2+} signals in sensory

neurons and introduce new therapeutic strategies for the prevention of paclitaxel-induced peripheral neurotoxicity by targeting the pathophysiological relevant Ca^{2+} dyshomeostasis.

Acknowledgements

We would like to thank Catherine Aubel for help in text editing and Petra Loge for excellent technical assistance. The research leading to these results has received funding from the federal ministry of education and research via the grant Center for Stroke Research Berlin (01 EO 0801) and Deutsche Forschungsgemeinschaft DFG (SFB TRR 43 to Matthias Endres and the EXC 257 Cluster of Excellence NeuroCure). W. Boehmerle and P. Huehnchen receive funding from the Charité Clinician Scientist Program funded by the Charité Universitätsmedizin Berlin and the Berlin Institute of Health. $InsP_3R1$ antibodies were a kind gift of Dr. B. Ehrlich. Plasmids for HM_3D and HM_4D DREADD expression were a kind gift of Dr. B.L. Roth and we acknowledge Dr. D. Trono

for addgene plasmids 12259 and 12260 (pMD2.G and psPAX2) and Dr. D. Baltimore for addgene plasmids 14883 (pFUGW).

Competing financial interests

The authors declare no competing financial interests.

Appendix A. Supplementary data

Supplementary data to this article can be found online at <https://doi.org/10.1016/j.expneurol.2018.04.014>.

References

- Alessandri-Haber, N., Dina, O.A., Yeh, J.J., Parada, C.A., Reichling, D.B., Levine, J.D., 2004. Transient receptor potential vanilloid 4 is essential in chemotherapy-induced neuropathic pain in the rat. *J. Neurosci.* 24, 4444–4452.
- Alessandri-Haber, N., Dina, O.A., Joseph, E.K., Reichling, D.B., Levine, J.D., 2008. Interaction of transient receptor potential vanilloid 4, integrin, and SRC tyrosine kinase in mechanical hyperalgesia. *J. Neurosci.* 28, 1046–1057.
- Armbruster, B.N., Li, X., Pausch, M.H., Herlitze, S., Roth, B.L., 2007. Evolving the lock to fit the key to create a family of G protein-coupled receptors potentially activated by an inert ligand. *Proc. Natl. Acad. Sci. U. S. A.* 104, 5163–5168.
- Arniges, M., Fernandez-Fernandez, J.M., Albrecht, N., Schaefer, M., Valverde, M.A., 2006. Human TRPV4 channel splice variants revealed a key role of ankyrin domains in multimerization and trafficking. *J. Biol. Chem.* 281, 1580–1586.
- Basbaum, A.I., Bautista, D.M., Scherrer, G., Julius, D., 2009. Cellular and molecular mechanisms of pain. *Cell* 139, 267–284.
- Berridge, M.J., 1998. Neuronal calcium signaling. *Neuron* 21, 13–26.
- Berridge, M.J., Bootman, M.D., Lipp, P., 1998. Calcium—a life and death signal. *Nature* 395, 645–648.
- Berridge, M.J., Bootman, M.D., Roderick, H.L., 2003. Calcium signalling: dynamics, homeostasis and remodelling. *Nat. Rev. Mol. Cell Biol.* 4, 517–529.
- Boehmerle, W., Endres, M., 2011. Salinomycin induces calpain and cytochrome c-mediated neuronal cell death. *Cell Death Dis.* 2, e168.
- Boehmerle, W., Splittgerber, U., Lazarus, M.B., McKenzie, K.M., Johnston, D.G., Austin, D.J., Ehrlich, B.E., 2006. Paclitaxel induces calcium oscillations via an inositol 1,4,5-trisphosphate receptor and neuronal calcium sensor 1-dependent mechanism. *Proc. Natl. Acad. Sci. U. S. A.* 103, 18356–18361.
- Boehmerle, W., Zhang, K., Sivula, M., Heidrich, F.M., Lee, Y., Jordt, S.E., Ehrlich, B.E., 2007. Chronic exposure to paclitaxel diminishes phosphoinositide signaling by calpain-mediated neuronal calcium sensor-1 degradation. *Proc. Natl. Acad. Sci. U. S. A.* 104, 11103–11108.
- Boehmerle, W., Huehnchen, P., Peruzzaro, S., Balkaya, M., Endres, M., 2014a. Electrophysiological, behavioral and histological characterization of paclitaxel, cisplatin, vincristine and bortezomib-induced neuropathy in C57BL/6 mice. *Sci. Rep.* 4, 6370.
- Boehmerle, W., Muenzfeld, H., Springer, A., Huehnchen, P., Endres, M., 2014b. Specific targeting of neurotoxic side effects and pharmacological profile of the novel cancer stem cell drug salinomycin in mice. *J. Mol. Med. (Berlin, Germany)* 92, 889–900.
- Bolte, S., Cordeliers, F.P., 2006. A guided tour into subcellular colocalization analysis in light microscopy. *J. Microsc.* 224, 213–232.
- Chen, Y., Yang, C., Wang, Z.J., 2011. Proteinase-activated receptor 2 sensitizes transient receptor potential vanilloid 1, transient receptor potential vanilloid 4, and transient receptor potential ankyrin 1 in paclitaxel-induced neuropathic pain. *Neuroscience* 193, 440–451.
- Clapham, D.E., 2003. TRP channels as cellular sensors. *Nature* 426, 517–524.
- Costa, R., Bicca, M.A., Manjavachi, M.N., Segat, G.C., Dias, F.C., Fernandes, E.S., Calixto, J.B., 2017. Kinin receptors sensitize TRPV4 channel and induce mechanical hyperalgesia: relevance to paclitaxel-induced peripheral neuropathy in mice. *Mol. Neurobiol.* <http://dx.doi.org/10.1007/s12035-12017-10475-12039>.
- Dardis, C., 2004. Peirce's criterion for the rejection of non-normal outliers: defining the range of applicability. *J. Stat. Softw.* 10, 1–8.
- Datwyler, A.L., Lattig-Tunnemann, G., Yang, W., Paschen, W., Lee, S.L., Dirnagl, U., Endres, M., Harms, C., 2011. SUMO2/3 conjugation is an endogenous neuroprotective mechanism. *J. Cereb. Blood Flow Metab.* 31, 2152–2159.
- De Smedt, H., Missiaen, L., Parys, J.B., Henning, R.H., Sienaert, I., Vanlingen, S., Gijssens, A., Himpens, B., Casteels, R., 1997. Isoform diversity of the inositol trisphosphate receptor in cell types of mouse origin. *Biochem. J.* 322 (Pt 2), 575–583.
- Delmas, P., Brown, D.A., 2002. Junctional signaling microdomains: bridging the gap between the neuronal cell surface and Ca²⁺ stores. *Neuron* 36, 787–790.
- Deng, H.X., Klein, C.J., Yan, J., Shi, Y., Wu, Y., Fecto, F., Yau, H.J., Yang, Y., Zhai, H., Siddique, N., Hedley-Whyte, E.T., Delong, R., Martina, M., Dyck, P.J., Siddique, T., 2010. Scapulo-peroneal spinal muscular atrophy and CMT2C are allelic disorders caused by alterations in TRPV4. *Nat. Genet.* 42, 165–169.
- Dunn, K.M., Hill-Eubanks, D.C., Liedtke, W.B., Nelson, M.T., 2013. TRPV4 channels stimulate Ca²⁺ – induced Ca²⁺ release in astrocytic endfeet and amplify neurovascular coupling responses. *Proc. Natl. Acad. Sci. U. S. A.* 110, 6157–6162.
- Everaerts, W., Zhen, X., Ghosh, D., Vriens, J., Gevaert, T., Gilbert, J.P., Hayward, N.J., McNamara, C.R., Xue, F., Moran, M.M., Strassmaier, T., Uykul, E., Owsianik, G., Vennekens, R., De Ridder, D., Nilius, B., Fanger, C.M., Voets, T., 2010. Inhibition of the cation channel TRPV4 improves bladder function in mice and rats with cyclophosphamide-induced cystitis. *Proc. Natl. Acad. Sci. U. S. A.* 107, 19084–19089.
- Faul, F., Erdfelder, E., Buchner, A., Lang, G., 2009. Statistical power analyses using G*Power 3.1: tests for correlation and regression analyses. *Behav. Res. Methods* 41, 1149–1160.
- Fernandes, J., Lorenzo, I.M., Andrade, Y.N., Garcia-Elias, A., Serra, S.A., Fernandez-Fernandez, J.M., Valverde, M.A., 2008. IP3 sensitizes TRPV4 channel to the mechano- and osmotransducing messenger 5'-6'-epoxyeicosatrienoic acid. *J. Cell Biol.* 181, 143–155.
- Flatters, S.J., Bennett, G.J., 2004. Ethosuximide reverses paclitaxel- and vincristine-induced painful peripheral neuropathy. *Pain* 109, 150–161.
- Garcia-Elias, A., Lorenzo, I.M., Vicente, R., Valverde, M.A., 2008. IP3 receptor binds to and sensitizes TRPV4 channel to osmotic stimuli via a calmodulin-binding site. *J. Biol. Chem.* 283, 31284–31288.
- Grynkiewicz, G., Poenie, M., Tsien, R.Y., 1985. A new generation of Ca²⁺ indicators with greatly improved fluorescence properties. *J. Biol. Chem.* 260, 3440–3450.
- Huehnchen, P., Boehmerle, W., Endres, M., 2013. Assessment of paclitaxel induced sensory polyneuropathy with "Catwalk" automated gait analysis in mice. *PLoS One* 8, e76772.
- Huehnchen, P., Boehmerle, W., Springer, A., Freyer, D., Endres, M., 2017. A novel preventive therapy for paclitaxel-induced cognitive deficits: preclinical evidence from C57BL/6 mice. *Transl. Psychiatry* 7, e1185.
- Huizing, M.T., Keung, A.C., Rosing, H., van der Kuyf, V., ten Bokkel Huinink, W.W., Mandjes, I.M., Dubbelman, A.C., Pinedo, H.M., Beijnen, J.H., 1993. Pharmacokinetics of paclitaxel and metabolites in a randomized comparative study in platinum-pre-treated ovarian cancer patients. *J. Clin. Oncol.* 11, 2127–2135.
- Jin, X., Shah, S., Liu, Y., Zhang, H., Lees, M., Fu, Z., Lippiat, J.D., Beech, D.J., Sivaprasadarao, A., Baldwin, S.A., Zhang, H., Gamper, N., 2013. Activation of the Cl-channel ANO1 by localized calcium signals in nociceptive sensory neurons requires coupling with the IP3 receptor. *Sci. Signal.* 6, ra73.
- Johanning, F.W., Zochowski, M., Conway, S.J., Holmes, A.B., Koulen, P., Ehrlich, B.E., 2002. Distinct intracellular calcium transients in neurites and somata integrate neuronal signals. *J. Neurosci.* 22, 5344–5353.
- Kao, J.P., 1994. Practical aspects of measuring [Ca²⁺] with fluorescent indicators. *Methods Cell Biol.* 40, 155–181.
- Kilkenny, C., Browne, W., Cuthill, I.C., Emerson, M., Altman, D.G., 2010. Animal research: reporting in vivo experiments: the ARRIVE guidelines. *Br. J. Pharmacol.* 160, 1577–1579.
- Klein, C.J., Shi, Y., Fecto, F., Donaghy, M., Nicholson, G., McEntagart, M.E., Crosby, A.H., Wu, Y., Lou, H., McEvoy, K.M., Siddique, T., Deng, H.X., Dyck, P.J., 2011. TRPV4 mutations and cytotoxic hypercalcemia in axonal Charcot-Marie-Tooth neuropathies. *Neurology* 76, 887–894.
- Kobayashi, K., Yamanaka, H., Noguchi, K., 2013. Expression of ATP receptors in the rat dorsal root ganglion and spinal cord. *Anat. Sci. Int.* 88, 10–16.
- Landouere, G., Zdebek, A.A., Martinez, T.L., Burnett, B.G., Stanescu, H.C., Inada, H., Shi, Y., Taye, A.A., Kong, L., Munns, C.H., Choo, S.S., Phelps, C.B., Paudel, R., Houlden, H., Ludlow, C.L., Caterina, M.J., Gaudet, R., Kleta, R., Fischbeck, K.H., Sumner, C.J., 2010. Mutations in TRPV4 cause Charcot-Marie-Tooth disease type 2C. *Nat. Genet.* 42, 170–174.
- Materazzi, S., Fusi, C., Benemei, S., Pedretti, P., Patacchini, R., Nilius, B., Prenen, J., Cremonin, C., Geppetti, P., Nassini, R., 2012. TRPA1 and TRPV4 mediate paclitaxel-induced peripheral neuropathy in mice via a glutathione-sensitive mechanism. *Pflugers Arch.* 463, 561–569.
- Mielke, S., Sparreboom, A., Mross, K., 2006. Peripheral neuropathy: a persisting challenge in paclitaxel-based regimens. *Eur. J. Cancer* 42, 24–30 (Epub 2005 November 2015).
- Mo, M., Erdelyi, I., Szigeti-Buck, K., Benbow, J.H., Ehrlich, B.E., 2012. Prevention of paclitaxel-induced peripheral neuropathy by lithium pretreatment. *FASEB J.* 26, 4696–4709.
- Ouyang, K., Zheng, H., Qin, X., Zhang, C., Yang, D., Wang, X., Wu, C., Zhou, Z., Cheng, H., 2005. Ca²⁺ sparks and secretion in dorsal root ganglion neurons. *Proc. Natl. Acad. Sci. U. S. A.* 102, 12259–12264 (Epub 2005 Aug 12215).
- Pease-Raissi, S.E., Pazyra-Murphy, M.F., Li, Y., Wachter, F., Fukuda, Y., Fenstermacher, S.J., Barclay, L.A., Bird, G.H., Walensky, L.D., Segal, R.A., 2017. Paclitaxel reduces axonal Bclw to initiate IP3R1-dependent axon degeneration. *Neuron* 96, 373–386 (e376).
- Pin, C.L., Rukstalis, J.M., Johnson, C., Konieczny, S.F., 2001. The bHLH transcription factor Mist1 is required to maintain exocrine pancreas cell organization and acinar cell identity. *J. Cell Biol.* 155, 519–530.
- Rogan, S.C., Roth, B.L., 2011. Remote control of neuronal signaling. *Pharmacol. Rev.* 63, 291–315.
- Ross, S.M., 2003. Peirce's criterion for the elimination of suspect experimental data. *J. Eng. Technol.* 20, 38–41.
- Ryskamp, D.A., Witkovsky, P., Barabas, P., Huang, W., Koehler, C., Akimov, N.P., Lee, S.H., Chauhan, S., Xing, W., Renteria, R.C., Liedtke, W., Krizaj, D., 2011. The polymodal ion channel transient receptor potential vanilloid 4 modulates calcium flux, spiking rate, and apoptosis of mouse retinal ganglion cells. *J. Neurosci.* 31, 7089–7101.
- Schindelin, J., Arganda-Carreras, I., Frise, E., Kaynig, V., Longair, M., Pietzsch, T., Preibisch, S., Rueden, C., Saalfeld, S., Schmid, B., Tinevez, J.-Y., White, D.J., Hartenstein, V., Eliceiri, K., Tomancak, P., Cardona, A., 2012. Fiji: an open-source platform for biological-image analysis. *Nat. Methods* 9, 676.
- Schlecker, C., Boehmerle, W., Jeromin, A., DeGray, B., Varshney, A., Sharma, Y., Szigeti-Buck, K., Ehrlich, B.E., 2006. Neuronal calcium sensor-1 enhancement of InsP3 receptor activity is inhibited by therapeutic levels of lithium. *J. Clin. Invest.* 116, 1668–1674.
- Siau, C., Bennett, G.J., 2006. Dysregulation of cellular calcium homeostasis in

- chemotherapy-evoked painful peripheral neuropathy. *Anesth. Analg.* 102, 1485–1490.
- Soderberg, O., Gullberg, M., Jarvius, M., Ridderstrale, K., Leuchowius, K.J., Jarvius, J., Wester, K., Hydbring, P., Bahram, F., Larsson, L.G., Landegren, U., 2006. Direct observation of individual endogenous protein complexes in situ by proximity ligation. *Nat. Methods* 3, 995–1000.
- Strotmann, R., Schultz, G., Plant, T.D., 2003. Ca²⁺ – dependent potentiation of the nonselective cation channel TRPV4 is mediated by a C-terminal calmodulin binding site. *J. Biol. Chem.* 278, 26541–26549 (Epub 22003 Apr 26530).
- Verkhratsky, A., Fernyhough, P., 2008. Mitochondrial malfunction and Ca²⁺ dyshomeostasis drive neuronal pathology in diabetes. *Cell Calcium* 44, 112–122.
- Wang, M.S., Davis, A.A., Culver, D.G., Wang, Q., Powers, J.C., Glass, J.D., 2004. Calcipain inhibition protects against Taxol-induced sensory neuropathy. *Brain* 127, 671–679 (Epub 2004 Feb 2004).
- Watanabe, H., Vriens, J., Janssens, A., Wondergem, R., Droogmans, G., Nilius, B., 2003. Modulation of TRPV4 gating by intra- and extracellular Ca²⁺. *Cell Calcium* 33, 489–495.
- Wu, Z., Wang, S., Wu, I., Mata, M., Fink, D.J., 2015. Activation of TLR-4 to produce tumour necrosis factor-alpha in neuropathic pain caused by paclitaxel. *Eur. J. Pain* 19, 889–898.
- Xiao, W.H., Zheng, H., Zheng, F.Y., Nuydens, R., Meert, T.F., Bennett, G.J., 2011. Mitochondrial abnormality in sensory, but not motor, axons in paclitaxel-evoked painful peripheral neuropathy in the rat. *Neuroscience* 199, 461–469.
- Xu, H., Fu, Y., Tian, W., Cohen, D.M., 2006. Glycosylation of the osmosensitive transient receptor potential channel TRPV4 on Asn-651 influences membrane trafficking. *Am. J. Physiol. Ren. Physiol.* 290, F1103–1109.
- Yilmaz, E., Gold, M.S., 2015. Sensory neuron subpopulation-specific dysregulation of intracellular calcium in a rat model of chemotherapy-induced peripheral neuropathy. *Neuroscience* 300, 210–218.
- Zhang, K., Heidrich, F.M., DeGray, B., Boehmerle, W., Ehrlich, B.E., 2010. Paclitaxel accelerates spontaneous calcium oscillations in cardiomyocytes by interacting with NCS-1 and the InsP3R. *J. Mol. Cell. Cardiol.* 49, 829–835.